Candidate Lensing Events for Gaia

prepared by: R. L. Smart, L. Smith, A. Vecchiato
affiliation : INAF - Osservatorio Astrofisico di Torino
approved by: U. Bastian
authorized by: M.G. Lattanzi
reference: GAIA-C3-TN-OATO-RLS-008-1
issue: 1
revision: 1
date: 2015-10-06
status: Issued

Abstract

We present a list of low mass lensing candidates for the Gaia mission. We discuss the problems expected in the observation of these events and recommend the adoption of a special observing strategy in some cases during the period surrounding the actual event.

Document History

Issue	Revision	Date	Author	Comment
D	1	2014-09-20	RLS	Creation
D	1	2015-05-20	LS	Added new examples
D	1	2015-09-30	RLS	Cleaned up text

Contents

1 Introduction **4**

1.1 Objectives 4

1.2 References 4

1.3 Acronyms 5

2 Adopted relations **6**

2.1 Simplified Nearest Approach 6

2.2 Masses of M to Y Dwarfs 7

2.3 Estimates of the Gravitational Deflection 7

3 Published Lensing Events **8**

4 The VVV region **8**

4.1 The Catalog 8

4.2 Candidate Identification 9

4.3 The Candidates 9

5 The All Sky Search **9**

5.1 The Catalog 9

5.2 Candidate Identification 10

6 Selected Predicted Events **12**

6.1 BD+63 137 12

6.2 Proxima Centauri 13

6.3 IGSL 4041768597398772992 13

7 Conclusions **14**

1 Introduction

With the wealth of fundamental observational data being provided by Gaia (distances, multi epoch photometry, spectra, motions etc) our knowledge of the derived physical parameters (age, temperatures, compositions, masses etc) will be similarly enriched. Directly determined masses in particular will be a crucial physical parameters being one of the most important physical parameters for determining the evolution, luminosity and lifetime of stars and brown dwarfs. The masses of stars are directly related to their luminosities and with the huge increase in directly derived masses from Gaia this relation will be precisely calibrated. However, there is no direct relation for very low mass stars and brown dwarfs where the age is directly correlated; for example models predict a 7 Myr 9 Jupiter mass planet, a 90 Myr 30 Jupiter mass brown dwarf and an 8 Gyr 80 Jupiter mass low-mass star all have the same luminosity. Mass will become one of the most critical parameters to understand these objects and a large calibrating sample will be required.

The currently most used method for the direct determination of ultra cool dwarf masses is via the fitting of orbital motions of dwarfs in binary systems (e.g. Zapatero Osorio & Martín, 2004; Liu et al., 2008; Konopacky et al., 2010; Dupuy et al., 2010). There will be 1000s of brown dwarfs in close orbits around stars detected by Gaia Sozzetti (2014) of which some will provide precise mass estimates. Other methods for mass determination such as the difference between spectroscopic and astrometric radial velocities due to gravitational redshift is limited to higher mass objects such as white dwarfs (Gatewood & Russell, 1974). Another method is via gravitational lensing of a distant object by a foreground object Proft et al. (2011); Belokurov & Evans (2002). Here we discuss Ultra Cool Dwarf candidate lensing events that are predicted to occur during the Gaia mission.

1.1 Objectives

To identify lensing events during Gaia's lifetime that will benefit from special observing strategy to maximize the precision of the mass estimate obtained.

1.2 References

Belokurov, V.A., Evans, N.W., 2002, MNRAS, 331, 649, ADS Link

Dupuy, T.J., Liu, M.C., Bowler, B.P., et al., 2010, ApJ, 721, 1725, ADS Link

Gatewood, G., Russell, J., 1974, AJ, 79, 815, ADS Link

Konopacky, Q.M., Ghez, A.M., Barman, T.S., et al., 2010, ApJ, 711, 1087, ADS Link

Lang, K.R., 1992, *Astrophysical Data I. Planets and Stars.*

Lépine, S., Shara, M.M., 2005, AJ, 129, 1483, ADS Link

Liu, M.C., Dupuy, T.J., Ireland, M.J., 2008, ApJ, 689, 436, ADS Link

Proft, S., Demleitner, M., Wambsganss, J., 2011, A&A, 536, A50, ADS Link

Rojas-Ayala, B., Iglesias, D., Minniti, D., Saito, R.K., Surot, F., 2014, A&A, 571, A36, ADS Link

Sahu, K.C., Bond, H.E., Anderson, J., Dominik, M., 2014, ApJ, 782, 89, ADS Link

Salim, S., Gould, A., 2003, ApJ, 582, 1011, ADS Link

Smart, R.L., Nicastro, L., 2014, A&A, 570, A87, ADS Link

Smith, L., Lucas, P.W., Bunce, R., et al., 2014a, MNRAS, 443, 2327, ADS Link

Smith, L., Lucas, P.W., Burningham, B., et al., 2014b, MNRAS, 437, 3603, ADS Link

Sozzetti, A., 2014, MSAIt, 85, XX

Zapatero Osorio, M.R., Martín, E.L., 2004, A&A, 419, 167, ADS Link

1.3 Acronyms

The following table has been generated from the on-line Gaia acronym list:

Acronym	**Description**
AGIS	Astrometric Global Iterative Solution
CCD	Charge-Coupled Device
CDS	Centre de Donnes astronomiques de Strasbourg
ESF	European Science Foundation
GOST	Gaia Observation Scheduling Tool
GPS	Galactic Plane Survey
GREAT	Gaia Research for European Astronomy Training
IGSL	Initial Gaia Source List
LAS	Large Area Survey
LSF	Line Spread Function
NLTT	New Luyten Two Tenths
UKIDSS	UKIRT Infrared Deep Sky Survey
VVV	Vista Variables in the Via Lactea

2 Adopted relations

We examine different catalogs of high proper motion objects to identify possible candidate lensing events. Here we outline the relations adopted to identify close approaches, estimate candidate masses and the determination of the predicted gravitational lensing shift.

2.1 Simplified Nearest Approach

The first step is to find the time and distance of nearest approach for our target high proper motion objects. We take the simple case where the distance is given by:
$d(t) = \sqrt{(\delta_p - \delta_q)^2 + (\alpha_p cos(\delta_p) - \alpha_q cos(\delta_q))^2}$
where α, δ are the equatorial positions of objects p, q and $d(t)$ is the distance all at time t.

We consider just the window 2015 to 2022. The steps we follow are:

1) Find the positions of objects p and q at 2015 (α, δ) .

2) The time of closest approach is given by:

$$t = -\frac{(\mu_{\delta_p} - \mu_{\delta_q}) * (\delta_p - \delta_q) + (\mu_{\alpha_p} cos(\delta_p) - \mu_{\alpha_q} cos(\delta_q)) * (\alpha_p cos(\delta_p) - \alpha_q cos(\delta_q))}{(\mu_{\delta_p} - \mu_{\delta_q})^2 + (\mu_{\alpha_p} cos(\delta_p) - \mu_{\alpha_q} cos(\delta_q))^2} \quad (1)$$

where the positions are all at 2015 and t is then the time from that epoch.

3) The distance of closest approach is then:

$$d(t) = \sqrt{\frac{((\mu_{\alpha_p} cos(\delta_p) - \mu_{\alpha_q} cos(\delta_q)) * (\alpha_p cos(\delta_p) - \alpha_q cos(\delta_q)))^2 - ((\mu_{\delta_p} - \mu_{\delta_q}) * (\delta_p - \delta_q))^2}{(\mu_{\delta_p} - \mu_{\delta_q})^2 + (\mu_{\alpha_p} cos(\delta_p) - \mu_{\alpha_q} cos(\delta_q))^2}} \quad (2)$$

4) If time is outside the 2015 to 2022 window then distance of closet approach is simply:

$$d(2015 \text{ or } 2022) = \sqrt{(\delta_p - \delta_q)^2 + (\alpha_p cos(\delta_p) - \alpha_q cos(\delta_q))^2} \quad (3)$$

where the positions are at 2015 or 2022.

Each target is compared to all nearby objects (e.g. within an arcminute).

2.2 Masses of M to Y Dwarfs

Once candidates are found we require an estimate of the mass of the lens. For M0 to M7 we used Lang (1992) except in the case of VVV objects where the colors allow a better estimate based on Rojas-Ayala et al. (2014).

For the M7 to T8 dwarfs we obtained the BT_Settl models for 1 and 10 gyr objects and then compared the SpT to mass relation. We assign a numerical spectral type (Spt) from M7=7, M8=8 ... T8=28 then the mass in solar masses is well represented by the relations:

$$M_{1GYR} = 0.19085559 - 0.020370740 * SpT + 0.0010516266 * SpT^2 - 1.9409372e-05 * SpT^3 \quad (4)$$

$$M_{10GYR} = 0.20122619 - 0.024811216 * SpT + 0.0015395785 * SpT^2 - 3.0435869e-05 * SpT^3 \quad (5)$$

We only consider the higher (older) mass case (e.g. the most significant).

2.3 Estimates of the Gravitational Deflection

To estimate the gravitational deflection we follow the development in Proft et al. (2011). In this discussion the lens is a nearby object that passes in front of a (usually) distant object which we will refer to as the source.

The angular Einstein radius is then defined as:

$$\Theta_E = \sqrt{\frac{4GM}{c^2} . \frac{D_s - D_l}{D_s D_l}} \quad (6)$$

and

$$r_E = D_l \Theta_E \quad (7)$$

where D_s, D_l are the distance of the lens and the source.

$$\Theta_E = \sqrt{\frac{4GM}{c^2} . \frac{1}{D_l}(1 - \frac{D_l}{D_s})} \quad (8)$$

Assuming the source is much further than the lens ($D_s >> D_l$) so $\frac{D_l}{D_s} -> 0$ then:

$$\Theta_E = \sqrt{\frac{4GM}{c^2 D_l}} \tag{9}$$

Using the variables: c=$2.99 * 10^{10} cm/s$, G=$6.672 * 10^{-8} cm^3/gs^2$, M in solar masses ($M_\odot$, D_l in parsecs.Then Θ_E simplifies to:

$$\Theta_E = 90[\sqrt{\frac{M}{D_l}}] \tag{10}$$

Finally we define the unitless variable

$$\mu = \frac{\theta_s - \theta_l}{\Theta_E} \tag{11}$$

where $\theta_s - \theta_l$ is the angle between the lens and the source. The observed centroid shift is then given by:

$$\delta = (\frac{\mu}{\mu^2 + 2})\Theta_E \tag{12}$$

3 Published Lensing Events

From the Proft et al (2011) work we find there are 7 predicted significant lensing events that fall during the Gaia mission period. In Sahu et al. (2014) they predict a encounter of Proxima Centauri with a background star of G=20 around 2015/2016. We include this and the Proft sample for completeness in the first part of table 1.

4 The VVV region

4.1 The Catalog

The Vista Variables in the Via Lactea (VVV) survey currently has just over 4 years of observations of approximately 560 square degrees of the Galactic bulge and plane. Typically each source is observed 50-150 times in the Ks band. We have produced a proper motion catalog using the currently available Ks band data, which contains approximately 200 million unique sources. Our relative proper motion accuracy approaches 1 mas/yr for bright sources. We have identified 550 sources with accurate motions in excess of 0.2"/yr as candidate lenses. Additionally, the catalog offers Ks positions and proper motions of background sources with a similar accuracy. Using lens and background source astrometry from the same pipeline we minimize systematic errors which may be present in the data.

4.2 Candidate Identification

To identify candidate astrometric lensing events we first select background sources from the VVV pawprint catalog in which the lens candidate is furthest from the edge of the array. Note that each source is present in two pawprints. Background sources are selected if they are within a radius equal to 15 years of motion of a lens candidate. The positions of all sources in the VVV astrometric catalog are given at epoch 2012.0, taking into account any proper motion measured. We are therefore sensitive to astrometric lensing events occurring between 1997.0 and 2027.0, assuming no motion of the background sources. Each lens-background source candidate pair are then projected onto the equatorial tangent plane (ξ,η), the tangent point being the 2012.0 position of the background source. The time to the minimum separation of the two sources in years relative to the epoch of the positions is given in equation 13 derived from equations in section 2.1.

$$t(d_{min}) = -\frac{(\mu_{\eta,l} - \mu_{\eta,s})(\eta_l - \eta_s) + (\mu_{\xi,l} - \mu_{\xi,s})(\xi_l - \xi_s)}{(\mu_{\eta,l} - \mu_{\eta,s})^2 + (\mu_{\xi,l} - \mu_{\xi,s})^2} \tag{13}$$

The minimum expected separation that this corresponds to is given in equation 14.

$$d_{min} = \sqrt{\frac{((\mu_{\eta,l} - \mu_{\eta,s})(\xi_l - \xi_s) - (\mu_{\xi,l} - \mu_{\xi,s})(\eta_l - \eta_s))^2}{(\mu_{\eta,l} - \mu_{\eta,s})^2 + (\mu_{\xi,l} - \mu_{\xi,s})^2}} \tag{14}$$

Where the time of the minimum expected separation falls outside of the Gaia observation window, either 2015 or 2022, we take the closest expected separation at either of these epochs.

4.3 The Candidates

From the 543 lens candidates with proper motion $> 200\ mas\ yr^{-1}$ and proper motion uncertainties $< 10\ mas\ yr^{-1}$, we have identified 11 candidates which are expected to pass within $0.5''$ of a background source between 2015.0 and 2022.0. These are included in table 1 along with the estimated gravitational deflection.

5 The All Sky Search

5.1 The Catalog

Our candidate lenses from a wider literature search are $> 100\ mas\ yr^{-1}$ sources drawn from:

- The Smith et al. (2014b) proper motion catalog of the UKIDSS Large Area Survey;
- The 617 high proper motion sources identified in a search of the UKIDSS Galactic Plane Survey at $l > 60^\circ$ by Smith et al. (2014a);
- A list of known ultracool dwarfs compiled by J. Gagné[1] retrieved Sept. 23rd 2014 which includes proper motion from a variety of sources;
- The revised NLTT catalog (Salim & Gould, 2003); And the LSPM-North catalog (Lépine & Shara, 2005).
- The 543 high proper motion objects identified in the VVV survey (see Section 4.1) in order to search for lenses passing in front of objects that are heavily saturated in the VVV survey.

This selection produces a total of 146,460 lens candidates, although there are many duplicates. For the moment, we assume that the positions of the ultracool dwarfs compiled by J. Gagné are at epoch 2000.0. The true positions are likely to be at epoch 2000^{+10}_{-3} years, taking into account the surveys in which they were likely to be identified, and a final calculated epoch of minimum separation will differ accordingly. Assuming no motion of the background source, the value of the minimum separation should not change. It is beyond the scope of this short investigation to identify the position epochs of the entire list, though any promising candidates were later verified.

We used the Initial Gaia Source List (IGSL, Smart & Nicastro 2014) as our catalog of background sources. The IGSL is an all-sky compilation catalog of several previous surveys and contains a homogeneous list of positions, proper motions, and importantly an estimated Gaia G band photometry among other parameters.

5.2 Candidate Identification

We performed a $1'$ cross-match of the lens candidate positions to the IGSL using the CDS XMatch service[2], returning 2.5 million rows. We rejected any pairings to high proper motion background sources since we require the sources to be distant ($D_s \gg D_l$). Lens candidate positions were moved to epoch 2000 where necessary (i.e. the LAS, GPS, and VVV data), and for each lens-background source candidate pair the time to minimum expected separation and minimum expected separation were calculated using equations 1 and 2 respectively.We rejected any lens-background source candidate pairings with epoch of minimum separation outside of 2015 to 2030, or minimum separation $> 1''$.

[1] http://jgagneastro.wordpress.com/list-of-ultracool-dwarfs/
[2] http://cdsxmatch.u-strasbg.fr/xmatch

Candidate Lensing Events

Published events Lens' Name	α_l, δ_l	$\mu_\alpha \cos\delta_l, \mu_{\delta,l}$ mas/yr	G_l	D_l pc	M_l $M_\odot$	G_s	Δ_{min} mas	Epoch Year	Def. mas
UCAC3 78-184250	13:45:41.45,-51:01:00.6	109.6,-515.5	14.7	118	0.5	17.9	110	2012.10	0.30
LP 344-7	22:26:56.82,+29:13:30.4	0.221,0.058	12.7	120	0.5	12.7	241	2014.52	0.15
OGLE BUL-SC36 490395	18:05:33.67,-28:11:29.1	-62.05,-175.2	18.8	107	0.5	19.4	122	2012.54	0.28
G 125-33	19:48:24.29,+32:50:32.7	0.133,0.169	13.5	239	0.5	14.2	3	2015.42	1.50
GJ 169.1 B	04:31:12.57,+58:58:41.1	1.336,-1.963	8.9	5	1	19.7	140	2014.03	9.10
LHS 5050	02:07:03.83,+49:38:44.1	0.237,-0.434	10.6	15	0.3	16.6	54	2015.77	2.85
G 125-56	20:04:20.93,+38:08:29.1	-0.169,-0.296	12.6	64	0.8	12.5	369	2015.62	0.26
2M2022+26	20:22:26.74,+26:57:09.5	-0.118,-0.313	15.1	152	0.5	17.0	111	2018.01	0.23
G 11-41	12:09:28.34,+00:42:14.1	-0.388,-0.025	13.8	104	0.5	17.2	168	2016.85	0.22
Proxima Cen	14:29:42.94,-62:40:46.1	-3775.75,765.54	9.9	1	0.2	18.1	1779	2014.90	0.73
Proxima Cen	14:29:42.94,-62:40:46.1	-3775.75,765.54	9.9	1	0.2	20.0	838	2015.76	1.55
All sky search Simbad Name	α_l, δ_l	$\mu_\alpha \cos\delta_l, \mu_{\delta,l}$	G_l	D_l	M_l	G_s	Δ_{min}	Epoch	Def.
BD+63 137	01:07:08.20, +63:56:28.8	1546, 318	8.4	15	0.7	18.9	88	2015.57	3.77
LHS 137	01:07:47.84, +34:12:30.6	1370, 479	12.2	26	0.3	18.9	36	2018.65	2.47
NLTT 6384	01:54:20.20, +08:57:37.1	-131, -119	13.9	43	0.3	20.3	20	2021.42	2.01
G 73-13	02:00:17.87, +04:13:01.6	-114, -182	13.6	90	0.3	13.4	38	2015.49	0.76
HD 27983	04:24:41.93, -08:45:12.0	-130, -167	8.3	51	1.1	16.2	22	2019.11	4.47
HD 39194	05:44:31.92, -70:08:36.9	-309, 1239	7.7	26	0.8	19.5	12	2019.64	5.55
LP 838-25	06:14:16.36, -23:10:22.5	190, -336	9.1	122	0.2	16.0	109	2016.66	0.12
2M0646+13	06:46:19.50, +13:04:47.2	129, -246	14.7	112	0.2	17.7	75	2017.15	0.19
2M0830+13	08:30:23.09, +13:43:09.7	53, -169	14.9	51	0.2	18.9	3	2017.16	2.03
BD+30 2129	11:17:03.55, +29:19:24.5	19, -180	9.7	134	0.6	12.5	23	2015.11	1.28
NLTT 35465	13:51:29.15, +03:24:27.2	107, -346	16.5	13	0.2	20.5	6	2019.75	4.10
BD+03 2855	14:06:17.53, +03:14:08.7	-328, -4	9.8	46	0.5	20.1	48	2019.77	1.68
LSPM1502+3531	15:02:11.81, +35:31:53.5	-322, -236	18.1	190	0.2	19.9	96	2018.84	0.09
2M1651+36	16:51:38.10, +36:56:52.1	-106, 132	17.2	138	0.2	18.3	56	2021.62	0.21
VVV1750-27	17:50:56.95, -27:23:36.9	-93, -258	15.1	81	0.2	15.0	64	2021.51	0.32
LHS 3335	17:52:48.82, -34:38:43.2	-430, -435	13.0	20	0.2	17.9	46	2020.66	1.70
EGGR 582	21:38:46.19, +23:09:21.6	266, 125	15.1	44	1.5	20.7	25	2020.89	5.89
BD+21 4948	23:32:22.62, +21:59:09.4	195, 37	10.2	151	1.1	12.2	63	2017.09	0.92
HIP 116810	23:40:28.99, +29:59:12.0	200, 2	10.6	64	0.4	14.5	51	2019.77	0.87
VVV Region IGSL sourceID	α_l, δ_l	$\mu_\alpha \cos\delta_l, \mu_{\delta,l}$	G_l	D_l	M_l	G_s	Δ_{min}	Epoch	Def.
4037219058697004800	17:55:51.40, -37:32:06.9	-111, -447	14.2	265	0.3	15.0	418	2018.32	0.01
4043906219826057728	18:00:27.41, -31:17:49.7	-1 , -232	19.0	90	0.4	17.3	284	2020.62	0.10
4041768597398772992	17:47:14.10, -33:58:03.5	-243, -282	18.4	38	0.2	17.5	442	2017.89	0.09
4063733644129995648	17:50:56.86, -27:23:40.0	-93 , -258	17.1	71	0.06	15.0	72	2020.59	0.07
4067945907534387200	17:44:17.80, -25:02:50.5	-4 , -233	14.3	69	0.2	14.3	394	2022.00	0.06
4116863214253975552	17:43:37.22, -23:04:05.3	-86 , -478	18.7	118	0.06	16.4	159	2020.51	0.03
5858969775597248512	13:12:01.57, -64:40:32.0	-335, 181	15.0	72	0.2	16.1	185	2021.56	0.12
5883622990960689280	15:32:38.34, -55:47:47.0	-147, -138	15.3	67	0.2	16.2	177	2021.88	0.14
5883613645106117376	15:34:20.95, -55:51:03.5	196 , 51	17.3	61	0.2	16.1	448	2022.00	0.06
5989792177328625152	16:16:23.01, -48:00:01.5	85 , -222	19.0	248	0.3	16.7	124	2020.27	0.08

6 Selected Predicted Events

Using the Gaia Observation Schedule Tool (GOST) [3] we have examined expected Gaia observations of some candidate events from table 1. To observe an event there are a number of considerations to evaluate, for example:
1) The Gaia scanning law means the observations are quite unevenly spaced and obviously independent of any lensing event.
2) The relative orientation of the gravitational deflection and the scanning direction impacts the precision with which we can measure any signal.
3) In general the lenses are close to bright stars and hence are subject to gating in the Gaia readout strategy - if the source is faint and within the same column as the lens we may not get a strong enough signal to be detected by Gaia.
4) If the lens is very bright then there will be diffraction spikes that may impact any centroiding of the fainter source - indeed the diffraction spikes, by their nature as a reflection of the mirror, are aligned to the along and across scan direction.
The consideration of a few of the events will illustrate some of the difficulties.

6.1 BD+63 137

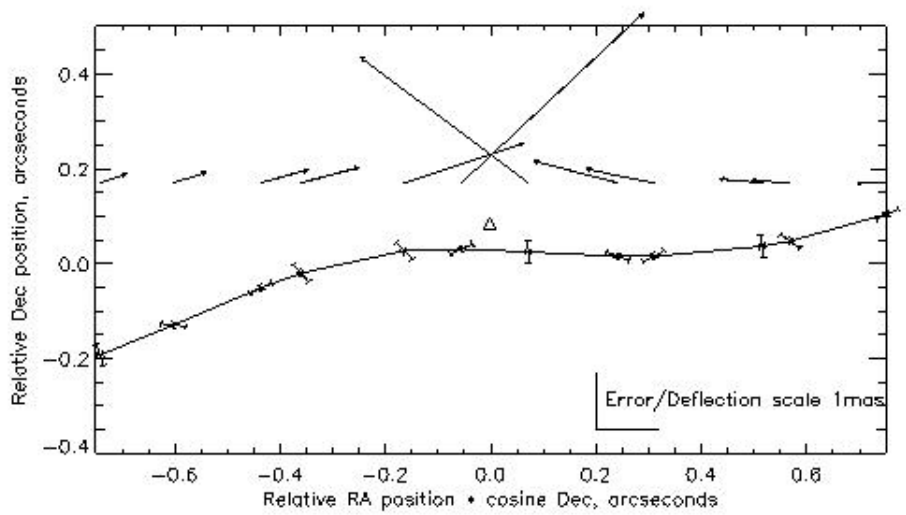

FIGURE 1: The predicted lensing event of BD+63 137. The wavy line is the motion of BD+63 137 with error bars representing Gaia precision at the predicted observations, the triangle is the background source and the arrows represent the predicted astrometric deflection of the source at the various observation epochs of Gaia.

We have looked at the candidate event of BD+63 137 which has 12 predicted Gaia observations over the 6 months centered on the predicted closest approach. In figure 1 we plot the motion

[3] http://gaia.esac.esa.int/tomcat_gost/gost/index.jsp

of BD+63 137 with respect to the source as a curved path. The squares represent the predicted Gaia observations where, adopting the GOST "Scan Angle" direction we plot the predicted error in along and across scan centroiding precision. We have assumed the single CCD centroiding precision described in the Gaia Science Performance [4] page. On the same graph, and in the same scale as the precision bars, we have plotted the expected deflection of the background source. In the case of this encounter the signal for all observations is 8-10 times the along scan precision and at only one point is the across scan position more significant.

The lens is very bright, G 8.4 so a full 2-d window will be downloaded for each observation. The scale of the figure is about the same as the Gaia window that will be downloaded so the source will always be in the same window or very close to it's edge so it will be difficult to observe due to the gating strategy of Gaia. The source has a magnitude of G 18.9 so given the shorter effective exposure time allotted it will probably not be detectable but if it is then it should be resolvable even at the closest approach of a .1 arcsecond.

6.2 Proxima Centauri

Proxima Centauri is predicted to encounter a background object in early 2016 Sahu et al. (2014). During the 6 months centered on this encounter Gaia is scheduled to observe the field 20 times. The delta magnitude is very high as in the case of BD+63 137 but the closest approach is not very small (0.6") the dominating reason we still see a large deflection is because the lens is very close to us. In this case the source will not be within the window of the lens but being faint (G 20) we will nominally only download the Line Spread Function (LSF). The gating strategy means when the source is in the same columns as the lens it will again have an effectively reduced exposure time, however when the source is "proceeding" or "following" the lens this will not occur and we should get the maximum precision in the centroiding as the along centroiding is in the direction of the gravitational deflection. This is also unfortunately where the diffraction spikes are the strongest and probably for a object this close to the Gaia limit the noise due to stray light on the centroiding, assuming it is still possible to detect the object, will be quite high. Nevertheless this event should be a good test and, if successful, scientific verification of the relative astrometric precision of Gaia. For the period around the event it may improve precision if Gaia makes 2-d window observations of the source and surrounding stars to be able to exploit both the most precise across scan position as well as the along scan ones.

6.3 IGSL 4041768597398772992

During the 6 months centered on the predicted lensing event by this object (2017.89) the current GOST forecast is for 16 observations. The predicted deflection is at a level of 3-4 sigma but that subject to change as it is based on photometrically derived masses and distances and proper motions of medium precision. As both the lens and source are faint they will only nominally be

[4] `http://www.cosmos.esa.int/web/gaia/science-performance`

observed in the LSF mode by Gaia. To obtain the highest precision in the gravitational deflection direction it would be better to have 2-d windows for both the lens, source, and nearby objects to use as fiducial points for a relative solution for the period surrounding the predicted event. Since this event is in 2017 it will also be possible to update the parameters of the prediction in particular after the first AGIS solutions allows an estimate of the relative motions from the more precise Gaia observations.

7 Conclusions

With some more effort on searching for predicted events it is possible to evaluate on a case-by-case basis and isolate those cases where the across scan position adds significant information, e.g. when the scan direction and the gravitational deflection are not aligned and when the lensing object is too faint for Gaia hence the vector between the lens and the source is not defined. In these cases it would be important to download 2-d windows for the lens, source and nearby reference objects to enable a precise calculation of both the along and across scan positions. This will be a high priority when Gaia produces the first all sky catalogs of astrometric parameters thus allowing an in-depth data-mining of a precise homogeneous dataset.

The work was carried out with the support of GREAT ESF grant 6867.